International Journal of Thin Films Science and Technology

http://dx.doi.org/10.18576/ijtfst/140101

Electrical Properties of Selenium Tellurium Chalcogenide Glass Doped with Antimony

A. Z. Mahmoud[1,2], *Lamiaa Galal Amin*[3], *Safwat A. Mahmoud*[3,4], *Mnahil. M. Bashier*[5], *Mohamed E. M. Eisa*[3], *N. Dhahri*[3], *Asma Mohamed*[5], *Safwa Yagoub*[3], *M. A. Abdel-Rahim*[2]

[1] Department of Physics, College of Science, Qassim University, Buraydah 52571, Saudi Arabia
[2] Department of Physics, Faculty of Sciences, Assiut University, Assiut 71516, Egypt
[3] Physics Department, Faculty of Science, Northern Border University, Arar, Saudi Arabia
[4] Center for Scientific Research and Entrepreneurship, Northern Border University, Arar, 13211, Saudi Arabia
[5] Department of Mathematics, Faculty of Science, Northern Border University, Arar, Saudi Arabia

Received: 9 Jul. 2024, Revised: 19 Oct. 2024, Accepted: 24 Oct. 2024
Published online: 1 Jan. 2025

Abstract: This present research employs a comprehensive study of the structural, optical, and electrical properties of $Se_{85-x}Te_{15}Sb_x$ glassy alloys, where $x = 2.5, 5, 7.5, 10$, and 15 at.%. The synthesis of the glassy materials of $Se_{85-x}Te_{15}Sb_x$ is made through the conventional melt quenching method. $Se_{85-x}Te_{15}Sb_x$ thin films were then prepared on glass substrates, which were ultrasonically cleaned in acetone and then in distilled water, by thermal evaporation in the high vacuum of the order of 10^{-5} Torr. Regarding the as-deposited films of $Se_{85-x}Te_{15}Sb_x$ ($x = 2.5, 5$, and 7.5%), the electrical conductivities (σ) are determined for the temperature interval of 300-450 K. This work explores the relationship between composition and the density of localized state at the Fermi level ($N(E_f)$) as well as the activation energy for conduction (ΔE). Two types of conduction mechanisms are distinguished, each being governed by different channels. Thus, the increase with temperature of σ at $(T > Tg)$ as exponential is related to localized states in the tails of conduction bands. On the other hand, conduction at $(T < Tg)$ takes place by variable range hopping of charged carriers within localized near the Fermi level states. With the increase of the annealing temperature, both electrical conductivity and inversely proportional parameter (ΔE) increase. The thesis also highlights the impact of annealing on other electrical properties of $Se_{82.5}Te_{15}Sb_{2.5}$ films particularly where the films transform from the amorphous state to the crystalline phase.

Keywords: Thin film, Conductivity, Electrical properties, Amorphous, hopping distance

1 Introduction

Because amorphous materials have so many uses in contemporary technology, their scientific study is becoming increasingly significant. In principle, any chemical combination can be transformed into an amorphous solid, depending on how rapidly it cools down from a molten state. The lack of long-range translation regularity in amorphous substances complicates the evaluation of their underlying structure and physical characteristics. Conversely, these major local orders in the shorter length scale region (0-5 Å) show that these are not completely random although they lack long-range orders. These material systems may also exhibit an intermediate range order (IRO) or a medium-range order (MRO) at the length scale 5-20 Å alongside the degree of short-range order (SRO).

The exceptional glass-forming ability, ease of synthesis, Chalcogenide glasses' high transition temperature, and chemical stability have drawn a lot of interest. Part of the reason for the high level of interest is the potential for semiconductor devices due to their unique electronic switching characteristics [1] and the reversible, thermally induced amorphous-to-crystalline phase change that some compositions display [2,3,4,5]. Presented phase change materials (PCMs) displayed the amorphous and crystalline phases that show significant differences in optical reflectivity and electrical conductivity. This property has led to the discovery of raw materials for phase change memory materials (PCMM) which are used in non-volatile memories and rewritable optical disks. As an important instance of the

* Corresponding author e-mail: lamiaa.galal2@nbu.edu.sa

application of chalcogenide glasses, the non-volatile phase change has its wide application in large-capacity data storage devices including PCRAM, which writes data by electric pulses or optical methods [6,7,8,9].

When the PCM undergoes a phase transition from its amorphous to crystalline state by joule or laser heating, the PCRAM may operate. Of the amorphous chalcogenide alloys, selenium (Se) is the most preferred of the two because it is cheaper [10,11]. However, its disadvantage includes high viscosity sensitivity, short working life, and low sensitivity. These problems can be alleviated by the inclusion of Cu as well as Te in the Se glass because it increases the crystallization temperature and lowers the aging effect than the pure Se glass [12,13,14,15,16]. New observations show that Se–Te alloys are superior to amorphous Se for xerographic applications and that the addition of Se into Te alloys improves the corrosion characteristics [17]. It is discovered that the Se–Te alloys are beneficial in real-world applications. It is known that when Se is added to Te, Tc gets higher. As a result, these glasses ought to be stable throughout time and at different temperatures while being used. Several attempts have been undertaken [18,19,20] to increase the stability of Se–Te by adding a third element, however, one of the alloys' disadvantages is heat instability that causes crystallization. The third element's insertion also increases the area that can create glass. Observations show that the third element contributes to the formation of a cross-linked structure, which boosts the glass transition and crystallization temperature of the binary alloy [21,22].

It has been discovered that adding Sb to Se–Te enhances both photoconductivity and thermal stability [23,24,25]. From an application perspective, phase change random access memory (PCRAM) and xerography both employ Se–Te–Sb glasses [25]. Saraswat et al. [26,27] investigated the temperature dependence of dc conductivity and I-V characteristics for $Se_{85-x}Te_{15}Sb_x$ (x = 2, 4, 6, 8, and 10) glasses. The glass with 4 weight percent Sb has the largest current and maximum DC conductivity, they deduced from the I-V characteristics. The Poole-Frenkel type of conduction is suggested by the linear relationship between ln(I) and $V^{1/2}$.

Tripathi et al. [28] investigated the impact of the Sb additive on the dark- (σ_d) and photoconductivity ($\sigma_p h$) in amorphous $Se_{85-x}Te_{15}Sb_x$ ($x = 2-10$ with 2 steps) glasses. It was discovered that as the Sb concentration rises (up to 4 %), both d and ph rise while electrical activation energy falls. When Sb continues to rise over 4, the trend in all of these measures reverses. These findings are explained by the higher density of localized states in the mobility gap of Se–Te–Sb alloys.

Prashanth and Asokan [29] used DSC and electrical switching experiments, respectively, to investigate the thermal characteristics and electrical-switching behavior of $Se_{55-x}Te_{45}Sb_x$ ($2 < x \leq 9$) semiconducting chalcogenide glasses. It was discovered that adding Sb improves the stability and propensity for glass formation. The studied glasses' glass-transition and crystallization temperatures showed slight increases with Sb concentration. However, it turned out that the glasses showed electrical switching of the memory kind. Additionally, it was discovered that the addition of Sb causes the glasses' switching voltages to drop.

Fadel et al. [30] investigated the dc electrical conductivity dc for $Se_{85}Te_{15-x}Sb_x$ (x = 0, 2, 4, and 6) thin films in the temperature range of 297–333 K. It was discovered that adding Sb (2-4 at.%) boosted Tg and dc. As Sb increased more (Sb>4 at.%), Tg and dc both dropped. However, a memory type switching was seen in the current–voltage (I–V) characteristics curves. Threshold voltage (VT) increases linearly with increasing film thickness and decreases exponentially with temperature for all investigated film compositions.

The alternating-current (ac) conductivity and dielectric characteristics of $Se_{85}Te_{15-x}Sb_x$ (x = 0, 2, 4, and 6 at.%) thin films were investigated by Hegab et al. [31]. Energy-dispersive X-ray spectroscopy, differential scanning calorimetry, and X-ray diffraction were used to describe the films' structure. With a frequency range of 102 Hz to 105 Hz, the ac conductivity and dielectric characteristics were examined in the temperature range of 297 K to 333 K. According to the experimental findings, temperature, frequency, and Sb concentration all affect the ac conductivity, $\sigma_{ac}(\omega)$, and dielectric constant. This behavior was explained by correlated barrier hopping between centers, which creates intimate valence-alternation pairings. At the Fermi level, the density of localized states N(Ef) was calculated. It was discovered that as frequency increased, the activation energy $\Delta E(\omega)$ decreased. Over the ranges examined, it was discovered that the dielectric constant ε_1 and dielectric loss ε_2 increased with increasing temperature and decreased with increasing frequency. The Guintini equation was used to analyze the dielectric loss ε_2 and determine the maximum barrier height Wm for the films under study. For chalcogenide glasses, the figures align with those derived from Elliott's theory of charge carrier hopping across a possible barrier. It was also looked into how the parameters under study changed with the amount of Sb.

Saraswat et al. [32] investigated the DC electrical conductivity and I–V characteristics of glassy thin pellets of $Se_{85-x}Te_{15}Sb_x$ (where $x = 2, 4, 6, 8$, and 10 at. %). The I-V characteristics revealed that, in comparison to the other glass with x equal to 2, 6, 8, and 10 at.%, the glass with 4 at.% of Sb has the lowest resistance and the highest current. The compound formation between Se and Sb was studied to understand the dependence of DC conductivity on compositions. The conduction mechanism was, therefore, qualitatively analyzed with the Poole–Frenkel model of conduction. The samples' current-voltage measurements were ohmic at lower voltages, but because of the heat produced by the tests at those voltages, they were non-ohmic at higher ranges.

2 Experimental Techniques

Using the standard melt quenching method, bulk chalcogenide $Se_{85-x}Te_{15}Sb_x$ (where x = 2.5, 5, 7.5, 10, 15, and 25 at.%) is made. According to their atomic percentage, suitable quantities of high quality (99.999%) Se, Te, and Sb (from Aldrich UK) are weighed (10 gm total weight). A quartz glass ampoule containing the weighing components is sealed under a 10-4 Torr vacuum. The Heraus programmable tube furnace (type RO7115) is used to heat the sealed ampoule. The rate of heating is roughly 3–5 K/min. For 24 hours, the temperature is maintained at 950 K. It takes long synthesis durations and repeated melt rocking to get a uniform material composition. The molten components are then rapidly quenched in a mixture of cold water to produce a glassy sample. The energy dispersive spectroscopy (EDAX) method is used to examine the alloys. The alloys' atomic percentage ratios closely resemble those of their bulk sample.

3 Preparation of Thin Films

Clean glass substrates are used in a high vacuum coating device at room temperature to create thick films (Edwards E 306A, UK) and by thermal evaporation of source material at 10^{-5} Torv. As part of the substrate cleaning regimen, the specimens are exposed to chromic acid for a full day, followed by soapy and distilled water. The substrates are then ultrasonically cleaned in an alcohol bath, and heat treated at 373K to remove any remaining moisture or ethyl alcohol.

Practical deposition is carried out using a rate of 3 nm/s and the substrate with a rotation of about 20 rpm to make the film deposited to be homogenous and uniform. About 17 cm is the effectively maintained gap between the substrates and the evaporation boat.

The thickness of the film deposition is a very important factor that determines the resistivity as well as the structural and optical characteristics of a film. In this study, the film thickness is measured using a quartz crystal thickness gauge (FTM5, Edwards) [33].

Later, thick aluminum sheets with a 600 nm thickness are created using a thermal evaporation process to provide ohmic connections. This is made using a mask with the dimensions of the substrate, with a wire of width 0.2cm put between the electrodes.

The films are thermally annealed for 30 minutes in a Pyrex tube furnace while nitrogen gas flows at various temperatures. In fact, before electrodes are deposited, the thin films are thermally annealed for electrical conductivity tests.

4 Electrical Measurements

Planer geometry of the films is used for the electrical conductivity measurement and is shown in Fig. 1. Here L is the length $(0.2cm)$, B is the breadth $(\approx 2.4cm)$ and the thin film thickness is defined as d, so the area of the cross-section for current is $A = B \times d$. Two probe methods are used for these measurements. Figure 2 depicts the configuration utilized for these measurements. The film's conductivity is ascertained using the following equation:

$$\text{"film's conductivity"} = \frac{L}{R \times B \times d} \tag{1}$$

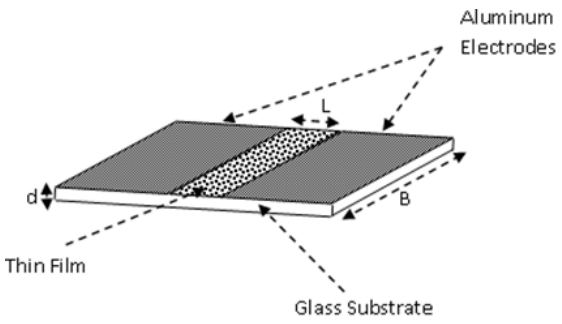

Fig. 1: Illustrates the partial deposition of the electrodes over the film.

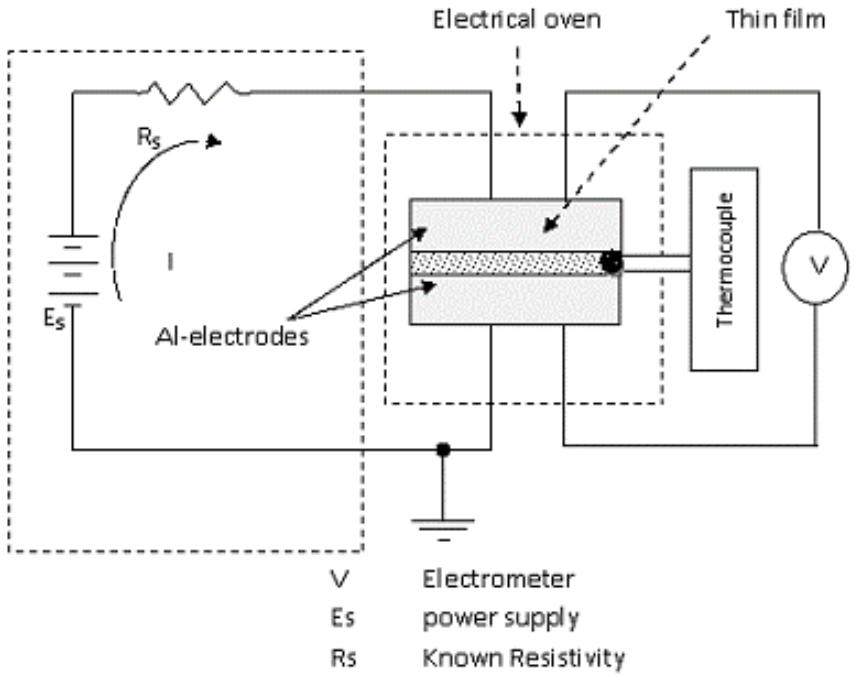

Fig. 2: Circuit schematic illustration for determining the thin-film electrical resistivity.

A Keithley 610 C electrometer is used to measure the electrical resistance values, R, according to temperature. These investigations are conducted at temperatures between 300 and 450 K, and they are conducted in the dark. A micro-voltmeter is used to measure the temperature using a calibrated copper constant thermocouple.

5 Sb Additive's Impact on Electrical Characteristics

It is investigated how the Sb concentration affects the DC electrical conductivity of as-deposited $Se_{85-x}Te_{15}Sb_x$ (x = 2.5, 5, and 7.5 at.%) films. The tests are performed on room-temperature glass substrates using films that are 250 nm thick. When the sample is heated from room temperature to 450 K, the electrical resistance is measured. The ln (σ) vs 1000/T curves for the as-deposited $Se_{85-x}Te_{15}Sb_x$ films are displayed in Fig. 3. According to the Arrhenius relation, electrical conductivity progressively rises with temperature in the first region (I), which spans from room temperature to the start crystallization temperature.

$$\sigma = \sigma_0 \exp\left(\frac{-\Delta E}{k_B T}\right) \tag{2}$$

where k_B, σ_0 and ΔE are the Boltzmann constant, the activation energy for conductance, and the pre-exponential factor, correspondingly.

The second region (II), corresponding to the change from amorphous to crystalline, exhibits a dramatic rise in the examined film's conductivity as a result of a modest temperature increase.

The Arrhenius equation (Eq. (2)) describes the relationship between electrical conductivity in the third region (III), which describes the crystalline states. As demonstrated by Mott [34], the electrical conduction mechanism may be ascertained with the use of the pre-exponential component, σ_0. According to Mott, conduction is in extended states if the pre-exponential factor value reported for a-Se and other Se alloyed films is on the order of $10^4(\Omega cm)^{-1}$. He demonstrated that conduction in the confined states in the band tails is indicated by a pre-exponential factor value that is two to three orders of magnitude lower [35,36,34]. Conduction in the localized states close to the Fermi level is indicated by even smaller values for σ_0 [37].

The first region (I) is referred to as the hopping conducting region by Mott. Conversely, the conduction in the confined states in the band tails is described by the third region (III).

Table 1: provides the values of electrical conductivity at the room temperature (σ_{RT}), activation energy (ΔE), and prefactor (σ_0) for $Se_{85-x}Te_{15}Sb_x$ films. These variations are symbolized by subscripts 1 and 2 for the low-temperature area and high-temperature area respectively.

Composition	$\sigma_{RT} \times 10^{-6}$	ΔE_1	σ_{01}	ΔE_2	σ_{02}
$Se_{82.5}Te_{15}Sb_{2.5}$	4.40	0.281	0.027	0.46	43.89
$Se_{80}Te_{15}Sb_5$	5.13	0.276	0.031	0.43	22.24
$Se_{77.5}Te_{15}Sb_{7.5}$	5.25	0.276	0.036	0.40	11.77

The deduced values ΔE, σ_0 and the electrical conductivity at room temperature, $\sigma_R T$, are listed in Table 1

It was found that the ΔE values declined as the σ values escalated as antimony content in the developed glasses increased. This means that the change in σ is accompanied by a similar change in ΔE. The examination of the variation in the resistivity of the films has shown that the decrease of resistivity at room temperature could be a result of the enhancement in the film quality by the reduction in the density of defect and slippage.

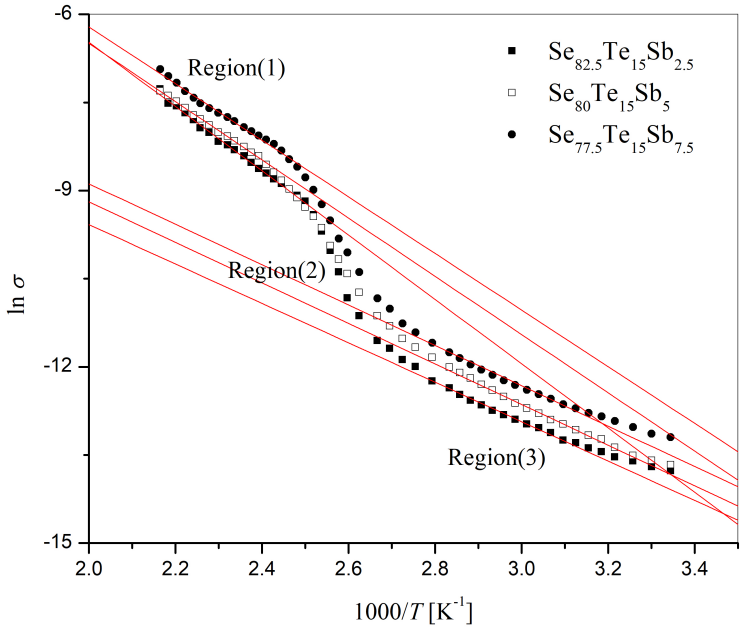

Fig. 3: The relation between ln σ versus 1000/T for the $Se_{85-x}Te_{15}Sb_x$ films.

Additionally, the metallic characteristics of Sb explain the contribution of direct conductivity DC and the related decrease in activation energy. The electron donor Sb behaves like a metal when it is introduced into the chalcogenide matrix and causes Fermi-level destabilization. By moving the Fermi level in the direction of the conduction band, these regions were discovered to generate an n-type conduction mechanism [38].

However, it is also noted that the increase in hopping conduction through defect states linked to the impurity atoms may be the origin of the conductivity increase [39]. Conduction takes place in either the confined states or the extended states above the mobility edge.

The measured conductivity is thought to be the sum of two elements, $\sigma = \sigma_{hop} + \sigma_{bt}$, where σ_{hop} is the conduction owing contribution to switching between the states that are localized and σ_{bt} is the contribution in band tails, to calculate the fermi-level density of localized states, N(Ef).

The electrical conductivity, σ, increases slightly with temperature below the glass transition point, which is consistent with transfer by hopping conduction. Conversely, the electrical conductivity, σ, grows exponentially with temperature, T, at $T > Tg$. It is possible to think of this rise as typical band-type conduction in band tails.

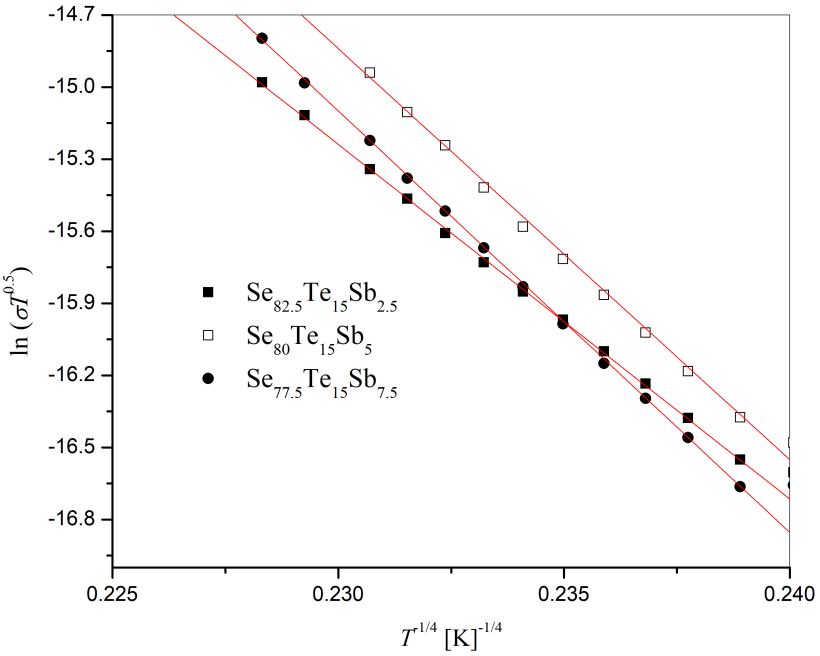

Fig. 4: ln $(\sigma T^{1/2})$ versus $T^{-1/4}$ plots for the $Se_{85-x}Te_{15}Sb_x$ films.

Table 2: Mott's parameters for the as-deposited $Se_{85-x}Te_{15}Sb_x$ films.

Composition	$\sigma_0^*(\Omega cm^{-1}K^{-0.5})$	$T_0 \times 10^8(K)$	$N(E_f) \times 10^{17}(cm^{-3}eV^{-1})$	$R \times 10^{-6}(cm)$	$W(ev)$
$Se_{82.5}Te_{15}Sb_{2.5}$	1.26×10^{10}	8.14	4.89	1.23	0.26
$Se_{80}Te_{15}Sb_5$	2.83×10^9	6.77	5.88	1.17	0.25
$Se_{77.5}Te_{15}Sb_{7.5}$	1.91×10^8	4.95	8.04	1.09	0.23

At a temperature of up to 350 K, varying with concentration, conduction occurs through variable range hopping of charge carriers amongst localized states in the vicinity of the Fermi level. This suggests that the charge transport is mediated by carriers hopping between localized states rather than through delocalized conduction bands). In this region, the conduction is characterized by Mott's relations Fig.4. illustrates the relation between $T^{-1/4}$ and ln $(\sigma T^{1/2})$ for the compositions under investigation. From a slope and where the straight lines connect, the values of To and σ_0 are determined and provided in Table 2. Also, the values of the density of localized states at the Fermi level N(Ef) are determined for the compositions under investigation and provided in Table 2. It is found from Table 2, that the values of the density of localized states N(Ef) increase with increasing the Sb content from 2.5 to 7.5 at. %. Since T_0 represents the degree of disorder, it follows that the amorphicity of the samples decreases with increasing Sb concentration. Furthermore, the pre-exponential factor σ_0^* decreases with increasing Sb content ensuring that the charge carrier mobility and density of states increase [40]. However, the highly electropositive Sb amplifies the Sb-Se bonds when it is added, introducing several faults into the system. Such change in ΔE is attributed to the progressive replacement of the stronger Se–Se bonds with a shorter bond energy of 44.04 kJ/mol by the Se–Sb bonds with a slightly lower bond energy of 43.98 kJ/mol. The increased density of the localized states is attributed to this substitution.

According to Mott [36] and Davis et. al. [35], two additional hopping parameters can be calculated: the hopping distance (R) [cm] and the hopping energy (W) [eV]. Table 2 presents the values of (R) and (W) determined for the films under investigation after these calculations have been completed. Table.2 shows that as the concentration of Sb increases, the values of W and R drop.

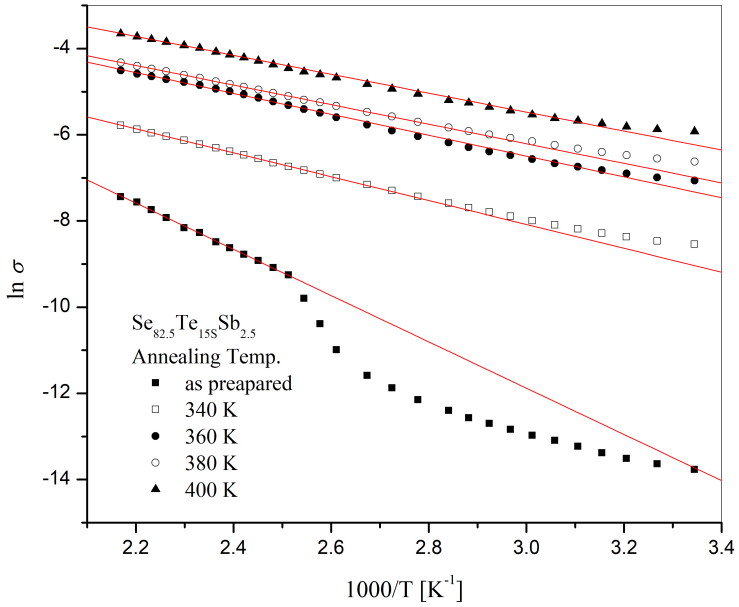

Fig. 5: The relation between 1000/T for $Se_{82.5}Te_{15}Sb_{2.5}$ and ln σ as-prepared and annealed films at different temperatures for 1 h.

Table 3: The activation energy for conduction, ΔE, and the electrical conductivity, σ, at 300 K for the as-deposited and annealed $Se_{82.5}Te_{15}Sb_{2.5}$ films.

Annealing Temp. [K]	$\sigma_{RT} \times 10^{-6}[\Omega\ \text{cm}]^{-1}$	ΔE_1[eV]
As-deposited	4.4×10^{-6}	0.46
340	2.84×10^{-4}	0.24
360	6.96×10^{-4}	0.21
380	8.74×10^{-4}	0.20
400	1.27×10^{-3}	0.19

6 Annealing Effect of the Electrical Properties of $Se_{82.5}Te_{15}Sb_{2.5}$

Measurements are made during heating from 300 to 450 K in order to examine the impact of the annealing temperature on the electrical conductivity of $Se_{82.5}Te_{15}Sb_{2.5}$ films. Figure 5 displays the dark electrical conductivity, σ, for the as-deposited and annealed films after one hour as a function of the reciprocal temperature. The electrical curve for the as-deposited film shows three regions with two distinct types of conduction pathways. However, the electrical curves of the annealed films show two distinct conduction pathways in addition to the conductivity's annealing dependency.

Figure 5 illustrates the relationship between ln (σ) and 1000/T in the high-temperature area. The slope of the straight lines in Equation (2) is used to determine the values of ΔE. Table.3 lists the electrical conductivity (Δ) and conduction activation energy (ΔE) for the as-deposited and annealed films, as determined at room temperature ($T = 300K$). The findings show that when annealing temperatures rise, electrical conductivity (σ) values rise and activation energy (ΔE) values fall. The amorphous–crystalline transition is responsible for this.

In the hopping region, figure 6 illustrates the relation between $\ln(\sigma/T^{0.5})$ and $(1/T^{0.25})$ of the as-deposited and annealed $Se_{82.5}Te_{15}Sb_{2.5}$ films. The data is in accordance with the Mott's variable-range hopping theory [41] plotting an appealing straight line between $\ln(\sigma/T^{0.5})$ and $(1/T^{0.25})$. The To values can be obtained from the slopes of the linear plots and the density of states N(Ef) at the Fermi level is determined for the as-prepared and annealed films and the results are summarized in Table 4. Additionally, the hopping distance R [cm] and the average hopping energy W [eV] for both film types are also computed in this work and presented in Table 4. From Table 4, it can also be noted that with an increase in annealing temperature, the T_0 values, which are related to the measurement of the state of disorder in the material, are reduced [42].

Table 4: Hoping parameters and the density of state localization $N\left(E_f\right)$ at the Fermi level for both asprepared and annealed $Se_{82.5}$ films with Te_{15} $Sb_{2.5}$.

Annealing Temp. [K]	σ_0^* $\left[\Omega cm^{-1}K^{0.5}\right]$	$T_0 \times 10^7$ [K]	$\boldsymbol{N\left(E_f\right)\times 10^{18}}$ $\left[\mathbf{cm^{-3}eV^{-1}}\right]$	$\boldsymbol{R\times 100^{-7}}$ [cm]	$\boldsymbol{W}$ [eV]
As-deposited	1.26×10^{10}	81.39	0.49	12.29	0.26
340	0.27×10^{6}	9.90	4.02	7.26	0.16
360	0.32×10^{6}	7.92	5.02	6.87	0.15
380	0.09×10^{6}	5.80	6.86	6.35	0.14
400	0.03×10^{6}	4.01	9.94	5.79	0.12

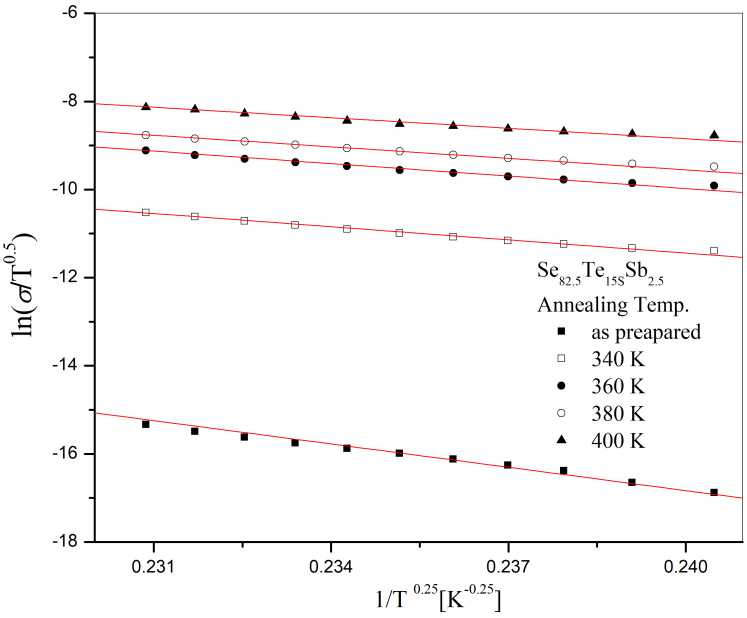

Fig. 6: The relation between $1/T^{0.25}$ for $Se_{82.5}Te_{15}Sb_{2.5}$ and $\ln(\sigma/T^{0.5})$ as-prepared and annealed films at different temperatures for 1 h.

7 Conclusions

Characterization of the amorphous transformation to crystalline states is carried by XRD and SEM; as the annealing temperature and the film thickness increase, the average crystallite size increases the dislocation density and strain decrease, respectively. The $Se_{85-x}Te_{15}Sb_x$ films (with $x = 2.5, 5$, and 7.5 at.%) show two different conduction modes, and the DC conductivity is increased with temperature. Conductivity σ and activation energy for conduction ΔE depend on composition; ΔE diminishes and σ raises with a higher content of Sb. Additionally, as Sb concentration rises, the number of molecules of state concentrated at the Fermi level rises while hopped distance and averaged hopping energy fall. As the annealing temperatures rise, the electrical conductivity rises while ΔE falls; concurrently, the density of localized states at the energy of Fermi, E_f, ($N(E_f)$), falls, and the hopping distance (R) and hopping energy (W) rise as well. Higher Sb concentration often improves SeTeSb's thermal and electrical performance, which in turn improves structural stability over time and temperature. This makes them suitable for use in xerographic and electrographic procedures, optical recording medium, and infrared spectroscopy.

Conflict of Interest

The authors declare that there is no conflict of interest regarding the publication of this paper.

References

[1] S. R. Ovshinsky, Reversible electrical switching phenomena in disordered structures, *Physical review letters* **21**(20) (1968) p. 1450.
[2] E. Evans, J. Helbers and S. Ovshinsky, Reversible conductivity transformations in chalcogenide alloy films, *Journal of Non-Crystalline Solids* **2** (1970) 334–346.
[3] J. Feinleib, J. DeNeufville, S. C. Moss and S. Ovshinsky, Rapid reversible light-induced crystallization of amorphous semiconductors, *Applied Physics Letters* **18**(6) (1971) 254–257.
[4] A. Smith, Twin coarsening in cdte (1 1 1) films grown on gaas (1 0 0), *Applied Optics* **13**(4) (1974) 795–798.
[5] M. Chen, K. A. Rubin and R. Barton, Compound materials for reversible, phase-change optical data storage, *Applied physics letters* **49**(9) (1986) 502–504.
[6] N. Yamada, E. Ohno, N. Akahira, K. Nishiuchi, K. Nagata and M. Takao, High speed overwritable phase change optical disk material, *Japanese Journal of Applied Physics* **26**(S4) (1987) p. 61.
[7] M. Wuttig and R. Waser, *Nanoelectronics and Information Technology* (Wiley Weinheim, 2003).
[8] M. Wuttig, Towards a universal memory, *Nature materials* **4**(4) (2005) 265–266.
[9] M. Wuttig and N. Yamada, Phase-change materials for rewriteable data storage, *Nature materials* **6**(11) (2007) 824–832.
[10] T. Ohta, K. Nishiuchi, K. Narumi, Y. Kitaoka, H. Ishibashi, N. Yamada and T. Kozaki, Overview and the future of phase-change optical disk technology, *Japanese Journal of Applied Physics* **39**(2S) (2000) p. 770.
[11] S. Ovshinsky, A new information paradigm–the ovonic cognitive computer": Bucharest, *Romania: INOE Publishing House: Non-Crystalline Materials for Optoelectronics* **1** (2004) 1–14.
[12] Z. Sun, J. Zhou and R. Ahuja, Structure of phase change materials for data storage, *Physical review letters* **96**(5) (2006) p. 055507.
[13] Z. Sun, J. Zhou and R. Ahuja, Unique melting behavior in phase-change materials for rewritable data storage, *Physical review letters* **98**(5) (2007) p. 055505.
[14] S. A. Khan, M. Zulfequar and M. Husain, On the crystallization kinetics of amorphous se80in20- xpbx, *Solid state communications* **123**(10) (2002) 463–468.
[15] N. Suri, K. Bindra, P. Kumar and R. Thangaraj, Non-cryst, *Solids* **353** (2007) p. 264.
[16] M. Abdel-Rahim, A. Gaber, A. Abu-Sehly and N. Abdelazim, Crystallization study of sn additive se–te chalcogenide alloys, *Thermochimica Acta* **566** (2013) 274–280.
[17] R. Chiba and N. Funakoshi, Crystallization of vacuum deposited te se cu alloy film, *Journal of non-crystalline solids* **105**(1-2) (1988) 149–154.
[18] M. Myers and E. Felty, Structural characterizations of vitreous inorganic polymers by thermal studies, *Materials Research Bulletin* **2**(7) (1967) 535–546.
[19] J. Schottmiller, M. Tabak, G. Lucovsky and A. Ward, The effects of valency on transport properties in vitreous binary alloys of selenium, *Journal of Non-Crystalline Solids* **4** (1970) 80–96.
[20] B. S. Patial, N. Thakur and S. Tripathi, Estimation of tg for se-te-sb system using modified gibbs-dimarzio law, *J. Therm. Anal. Calorim* **106** (2011) p. 845.
[21] I. Yahia, A. Shakra, M. Fadel, N. Hegab, A. Salem and A. Farid, Kinetics of non-isothermal crystallization of ternary se_{85} te_{15-x} sb_x glassy alloys., *Chalcogenide Letters* **8**(8) (2011).
[22] N. Maharjan, K. Singh and N. Saxena, Calorimetric studies in se_{75} te_{25-x} sn_x chalcogenide glasses, *physica status solidi (a)* **195**(2) (2003) 305–310.
[23] A. Gadkari and J. Zope, Electrical properties of the amorphous semiconducting se-te-in system, *Journal of non-crystalline solids* **103**(2-3) (1988) 295–299.
[24] P. Agarwal, S. Goel, J. Rai and A. Kumar, Calorimetric studies in glassy se_{80-x} te_{20} in_x, *physica status solidi (a)* **127**(2) (1991) 363–369.
[25] M. Mehdi, G. Brun, J. Jumas and J. Tedenac, Kinetic studies of the glass transition in (se 65 te 35) 100- x sb x by differential scanning calorimetry, *Journal of materials science* **30** (1995) 5732–5736.
[26] V. K. Saraswat, K. Singha and N. Saxena, Electrical measurements of se_{85-x} te_{15} sb_x glasses, *Indian Journal of Pure & Applied Physics* **44** (2006) 782–785.
[27] V. K. Saraswat, V. Kishore, N. Deepika Saxena *et al.*, Iv measurements of se-te-sb glassy bulk and thin film samples, *Chalcogenide Lett* **5**(5) (2008) 95–103.
[28] S. Tripathi, V. Sharma, A. Thakur, J. Sharma, G. Saini and N. Goyal, Effect of sb additive on the electrical properties of se–te alloy, *Journal of non-crystalline solids* **351**(30-32) (2005) 2468–2473.
[29] S. B. Prashanth and S. Asokan, Effect of antimony addition on the thermal and electrical-switching behavior of bulk se–te glasses, *Journal of non-crystalline solids* **355**(3) (2009) 164–168.
[30] M. Fadel, N. Hegab, I. Yahia, A. Salem and A. Farid, Electrical and switching properties of se85te15-xsbx ($0 \leq x \leq 6$ at. wt%) thin films, *Journal of alloys and compounds* **509**(29) (2011) 7663–7670.
[31] N. Hegab, M. Fadel, I. Yahia, A. Salem and A. Farid, Electrical conductivity and dielectric properties of se 85 te 15-x sbx ($x = 0$ at.%, 2 at.%, 4 at.%, and 6 at.%) thin films, *Journal of electronic materials* **42** (2013) 3397–3407.
[32] V. K. Saraswat, K. Singh, N. Saxena, V. Kishore, T. Sharma and P. Saraswat, Composition dependence of the electrical conductivity of se85-xte15sbx ($x = 2, 4, 6, 8$ and 10) glass at room temperature, *Current applied physics* **6**(1) (2006) 14–18.
[33] A. Hruby, Evaluation of glass-forming tendency by means of dta, *Czechoslovak Journal of Physics B* **22** (1972) 1187—-1193.

[34] N. Mott, Conduction in non-crystalline systems: Iv. anderson localization in a disordered lattice, *Philosophical Magazine* **22**(175) (1970) 7–29.
[35] E. Davis and N. Mott, Conduction in non-crystalline systems v. conductivity, optical absorption and photoconductivity in amorphous semiconductors, *Philosophical magazine* **22**(179) (1970) 0903–0922.
[36] N. Mott, E. Davis and R. Street, States in the gap and recombination in amorphous semiconductors, *Philosophical Magazine* **32**(5) (1975) 961–996.
[37] M. M. Khan, M. Zulfequar and M. Husain, Estimation of the density of localized states of a-se100- xbix films from electrical properties, *Physica B: Condensed Matter* **322**(1-2) (2002) 1–11.
[38] H. Fritzsche, P. Gaczi and M. Kastner, The effect of electronegativity difference on the defect chemistry in lone-pair semiconductors, *Philosophical Magazine B* **37**(5) (1978) 593–600.
[39] B. Kolomiets, E. Lebedev and N. Rogaciov, Impurity effect on electrical and optical properties of vitreous arsenic selenide, *Soviet Phys. Semiconductors* **8** (1974) 545–549.
[40] M. Abd El-Raheem, Electrical properties of gesetl thin films deposited by e-beam evaporation technique, *Materials Chemistry and Physics* **116**(2-3) (2009) 353–357.
[41] N. F. Mott, Conduction in non-crystalline materials: Iii. localized states in a pseudogap and near extremities of conduction and valence bands, *Philosophical Magazine* **19**(160) (1969) 835–852.
[42] E. Ebenezer, K. Murali, M. J. Chockalingam and V. Venkatesan, Electrical properties of vacuum annealed cds films, *Journal of materials science* **23** (1988) 3861–3863.